

Effect of wind and structural parameters on across wind load of super high-rise buildings

Ashish Singh, Sasankasekhar Mandal

Online Publication Date: 10 June 2023

URL: <http://www.jresm.org/archive/resm2023.727st0403.html>

DOI: <http://dx.doi.org/10.17515/resm2023.727st0403>

Journal Abbreviation: *Res. Eng. Struct. Mater.*

To cite this article

Singh A, Mandal S. Effect of wind and structural parameters on across wind load of super high-rise buildings. *Res. Eng. Struct. Mater.*, 2023; 9(4): 1459-1475.

Disclaimer

All the opinions and statements expressed in the papers are on the responsibility of author(s) and are not to be regarded as those of the journal of Research on Engineering Structures and Materials (RESM) organization or related parties. The publishers make no warranty, explicit or implied, or make any representation with respect to the contents of any article will be complete or accurate or up to date. The accuracy of any instructions, equations, or other information should be independently verified. The publisher and related parties shall not be liable for any loss, actions, claims, proceedings, demand or costs or damages whatsoever or howsoever caused arising directly or indirectly in connection with use of the information given in the journal or related means.



Published articles are freely available to users under the terms of Creative Commons Attribution - NonCommercial 4.0 International Public License, as currently displayed at [here](https://creativecommons.org/licenses/by-nc/4.0/) (the "CC BY - NC").



Research Article

Effect of wind and structural parameters on across wind load of super high-rise buildings

Ashish Singh^{*a}, Sasankasekhar Mandal^b

Department of Civil Engineering, IIT(BHU), Varanasi, India

Article Info

Abstract

Article history:

Received 03 Apr 2023

Accepted 07 June 2023

Keywords:

*Across wind equivalent static wind loads;
Super high-rise building;
Wind and Structural parameters.*

Designing a super high-rise building requires careful consideration of wind loads. The across wind load plays a critical role for super high-rise buildings. A super high-rise building's across-wind load is highly dependent on wind parameters as well as building parameters. It is still unclear how these parameters affect across wind load. Within a possible practical range, this paper attempts to measure the effect of wind and structural parameters on across wind load of a super high-rise building. The wind parameters considered in this study are exponent of mean velocity profile, turbulence intensity, background peak factor and, peak factor for resonant response. Structural parameters influencing across wind load are also considered, such as natural frequency, and structural damping ratio. An analytical method is employed to evaluate the across wind loads to carry out the study. From the results, it can be concluded that among the structural parameters, natural frequency of the structure is the most dominant parameter for the evaluation of across wind loads. In terms of wind parameters, the exponent of mean wind profile has the most impact on the across wind load. The across wind load is not affected by turbulence intensity. This study assists the designers in determining the most appropriate values for wind and structural parameters while estimating the across wind loads.

© 2023 MIM Research Group. All rights reserved.

1. Introduction

Scientific and technological advancements have led to structures becoming taller and slender, and more susceptible to strong winds. Tall buildings are typically subjected to wind loads determined by wind characteristics and aerodynamic properties. It is particularly difficult for tall buildings in coastal areas to withstand severe wind loads due to frequent cyclones. Tall buildings are subjected to dynamic loads due to the turbulent nature of wind. High-rise structures vibrate in a number of ways when exposed to wind, including torsional, across-wind, and along-wind motions. Windward and leeward pressure fluctuations cause along wind vibrations, which typically follow changes in the approach flow, particularly at low frequencies [1,2]. Alternatively, vortex shedding inside the wake zone or galloping can result in transverse or lateral aerodynamic behavior. Both can be attributed to incident turbulence and potentially triggered by turbulence-induced buffeting [3]. The wind-induced torsional load comes into the picture due to structural as well as architectural framework (non-symmetric cross-section, non-symmetrical mass & stiffness distribution) [4] or by wind flow characteristics (uneven pressure distribution across the face, flow approaching at an oblique angle to the face [5,6].

A wind tunnel study conducted by Gu and Quan [7] examined various factors affecting across wind loads on distinctive tall buildings. Studies indicate that across wind dynamic responses of super-tall structures sometimes might be greater than the along-wind ones

^{*}Corresponding author: ashishsingh.rs.civ18@iitbhu.ac.in

^a orcid.org/0000-0001-7907-6179; ^b orcid.org/0000-0002-5495-3793

DOI: <http://dx.doi.org/10.17515/resm2023.727st0403>

Res. Eng. Struct. Mat. Vol. 9 Iss. 4 (2023) 1459-1475

[7,8]. Zhou *et al.* [9] formulated a guideline to estimate equivalent static wind load (ESWL) on structures. The maximum acceleration of the Jin Mao building in the across wind direction is about 1.2 times that in the along wind direction at the design wind speed [10]. Li *et al.* [11] carried out full-scale study of the Jin Mao building and observed the dynamic response of the structure during typhoon Rananim. While the typhoon occurred, acceleration responses were generally higher in across wind directions when compared to the along-wind directions. The measured and calculated natural frequencies of the Jin Mao building differ nearby 10.6-17%. These studies indicate the importance of across wind load in high rise buildings. Zheng and Alex [12] conducted a comparative study on across wind loads on tall building with different codal provisions and discussed the Chinese code [13] in detail. They concluded that there is wide variability in defining the far field wind profile (wind spectrum, turbulence profile, turbulence integral scale and correlation) for specific locations calculated by various codal provisions. They also emphasized that a specific model from full-scale can reduce the significant uncertainty on the design wind load versus the design wind speed. Kwon and Kareem [14] examined the most important wind standards for tall buildings due to adverse wind implications. Holmes *et al.* [15] compared the wind loads for low, medium, and high-rise structures using fifteen distinct international codes.

Quan and Gu [16] have developed an analytical method to estimate the across wind ESWL of a super high-rise building. The term "super high-rise building" refers to buildings that are 300 meters or higher in height. Singh and Mandal [17] investigated the impact of plan and height aspect ratios on across wind loads using this analytical approach and contrasted it with along wind loads. A tall building's wind load is influenced by a number of structural, geometrical, and wind characteristics. The impact of geometrical characteristics on the across wind load through aerodynamic modification has been examined in a number of studies [18]. Many studies also discuss the influence of structural damping in reducing the across wind load [19].

Due to insufficient knowledge regarding the role of wind and structural parameters on across wind load, an analytical method is utilized to identify the effect of various parameters on across wind loads. Out of structural parameters, the Natural frequency of the structure (f) and structural damping ratio (ζ_s) are selected due to their key role in the calculation of across wind load. Four parameters (Exponent of mean velocity profile (α), turbulence intensity (I_H), peak factor for resonant response (g_R), and the background peak factor (g_B)) are selected out of wind parameters because of their significance in defining the characteristics of wind approaching the structure. Thus, the effects of these parameters on the across wind load are examined in this paper. A hypothetical 300 m super high-rise building with a square cross-section, assumed to be located in urban terrain, is adopted for the analysis. In order to comprehend the range of parameters, several international codes are used for each parameter evaluation. For suitability, we have referred to the codes that explicitly provided the corresponding parameters. Various international codes/ Standards have provided certain values of these parameters applicable to their specific site conditions. An understanding of how these parameters affect the across wind load will greatly assist engineers in accurately calculating the across-wind load for the structure. Accurate estimation of wind and structural parameters is essential because inaccurate estimation of these parameters will lead to underestimation or overestimation of across wind load. An incorrect load calculation will result in a faulty building design.

2. Analytical Method

Analytical method utilized in the study is derived from the wind tunnel studies. The analytical method calculates the across wind ESWL, based on the geometrical & structural configuration of the structure and approaching wind parameters. Quan and Gu [16]

provided detailed instructions to evaluate the across wind ESWL. The procedure to evaluate across wind load is described briefly in the following steps:

First the dimensions of the buildings *viz.* height(H), width(B) & Depth(D) must be determined then find out the structural parameters *viz.* fundamental frequency (f_i) of the building, structural damping ratio (ζ_s), first mode shape $\phi_i = (z/H)^\beta$. Mode shape index (β)=1. The equation (1) denotes the generalized mass, where, $m(z)$ = mass per unit height at height z .

$$M_i^* = \left[\int_0^H m(z) \times \phi_i^2(z) dz \right] \quad (1)$$

Acquire the wind related parameters *viz.* turbulence intensity (I_H), mean wind velocity profile exponent (α), The wind pressure exerted at the uppermost section of a building (w_H), and mean velocity at the top of the building (U_H).

Coefficient of background base moment (C_{M-B0}) is evaluated using equation (2).

$$C_{M-B0} = \{ 0.182 - 0.019\alpha_{db}^{-2.54} + 0.54\alpha_w^{-0.91} \} \quad (2)$$

Where, $\alpha_{db} = D/B$; eventually, it will ultimately turn into one since a square building is taken into consideration. α_w is function of turbulence intensity (I_H) expressed as

$$\alpha_w = 4.2 - 4e^{3.7-60I_H} \quad (3)$$

Davenport [1] proposed an empirical formula to evaluate the peak factor for resonant response (g_R) as shown in equation (4).

$$g_R = \sqrt{2 \ln(600f_1)} + \frac{0.5772}{\sqrt{2 \ln(600f_1)}} \quad (4)$$

$S_M^*(n)$ is expressed as

$$S_M^*(n) = \frac{S_p \eta (n/f_p)^\lambda}{\left\{ 1 - (n/f_p)^2 \right\}^2 + \eta (n/f_p)^2} \quad (5)$$

In equation (5), f_p = Location parameter, S_p = Amplitude parameter, η = bandwidth parameter, λ = deflection parameter and α_{hr} = height ratio, Reduced frequency(n) = $f B/U_H$. Equations (6) to (10) are employed to compute these factors.

$$S_p = \{ (0.1\alpha_w^{0.4} - 0.0004e^{\alpha_w}) \times (0.84\alpha_{hr} - 2.12 - 0.05\alpha_{hr}^2) \times (0.422 + \alpha_{db}^{-1} - 0.08\alpha_{db}^{-2}) \} \quad (6)$$

$$f_p = \{ 10^{-5} (191 - 9.48\alpha_w + 1.28\alpha_{hr} + \alpha_{hr}\alpha_w) \times (68 - 21\alpha_{db} + 3\alpha_{db}^2) \} \quad (7)$$

$$\eta = \{ (1 + 0.00473e^{1.7\alpha_w}) \times (0.065 + e^{1.26 - 0.63\alpha_{hr}}) e^{1.7 - 3.44/\alpha_{db}} \} \quad (8)$$

$$\lambda = \{ (-0.8 + 0.06\alpha_w + 0.0007e^{\alpha_w}) \times (-\alpha_{hr}^{0.34} + 0.00006e^{\alpha_{hr}}) \times (0.414\alpha_{db} + 1.67\alpha_{db}^{-1.23}) \} \quad (9)$$

$$\alpha_{hr} = H/\sqrt{BD} \quad (10)$$

The aerodynamic damping ratio ζ_a derived by Quan et al. [20] is computed as

$$\zeta_a = \frac{\{ 0.0025 (1 - (U^*/9.8)^2) (U^*/9.8) + 0.000125 (U^*/9.8)^2 \}}{\{ (1 - (U^*/9.8)^2)^2 + 0.0291 (U^*/9.8)^2 \}} \quad (11)$$

where, U^* = Reduced wind speed and expressed in equation (12).

$$U^* = [U_H / f_1 B] \tag{12}$$

The across wind ESWL, $\hat{p}(z)$ is calculated using equation (13), where, G_B = Background load coefficient, G_R = Resonant load coefficient, they are expressed in equations (14) & (15) respectively.

$$\hat{p}(z) = W_H B \sqrt{G_B^2(z) + G_R^2(z)} \tag{13}$$

$$G_B(h) = \{ (0.65 + 1.3h + 7h^2 - 7.5h^3) g_B C_{M-B0} \} \tag{14}$$

$$G_R(z) = \frac{H m(z)}{M_i^*} \left(\frac{z}{H} \right)^\beta g_R \sqrt{\frac{\pi \Phi S_M^*(f_1)}{4(\zeta_{s1} + \zeta_{a1})}} \tag{15}$$

Where, $\Phi=1$ for first mode [21], ζ_{s1} = Structural damping ratio, and ζ_{a1} = Aerodynamic damping ratio, accordingly for the first mode.

The peak acceleration can be calculated using equation (16).

$$\hat{a}(z) = \frac{H}{M_i^*} B g_R W_H \left(\frac{z}{H} \right)^\beta \sqrt{\frac{\pi \Phi S_M^*(f_1)}{4(\zeta_{s1} + \zeta_{a1})}} \tag{16}$$

3. Fixed Parameters of the Building

This research investigates a theoretical tall structure located within the city environment. The wind direction and the plan of the building are shown in Fig.1. The plan dimension, height & other parameters of the building which are kept constant throughout this study are enumerated in Table 1. A discussion of the parameters which are varied will follow in the next section.

Table 1. Building parameters that are kept constant throughout the study

H(m)	B(m)	D(m)	β	$M_1^*(\text{kg})$
300	50	50	1	$5.0 \cdot 10^7$

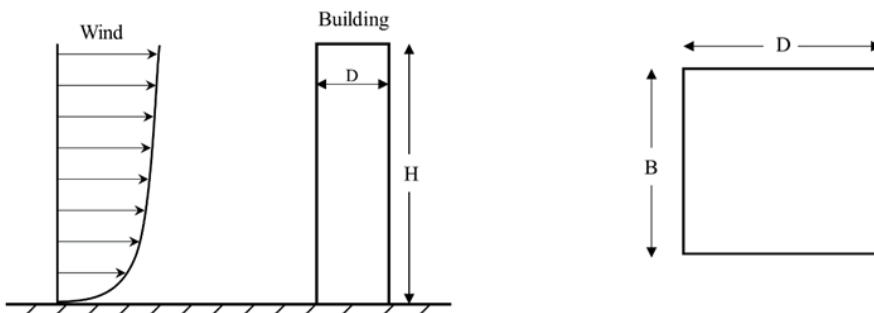


Fig. 1 Direction of wind and plan of the building

4. Structural Parameters

4.1 Natural Frequency of the Structure (f)

When it comes to determining wind loads, the natural period of a building holds the utmost importance. Table 2 shows the formulations available to calculate time period of tall RC buildings for wind design. The natural frequency of high-rise buildings with a height of H meter would be $f_1 = \frac{1}{T_1}$.

Natural time period is calculated according to the various codal provisions. There exists wide variability in the expressions for natural period provided by different codes and researchers. It is clearly visible from Table 2 that only Indian standard takes into account the base dimension in the formulation of time period. All other expressions are function of total height of the building only.

Table 2. Various recommendation of natural period (H & D are shown in Fig.1)

Code	Natural Time Period (T)	Natural Frequency (f)
ASCE 7-16 [22]	$T = H^{0.9}/43.5$	0.2565
Eurocode [23]	$T = 0.022H$	0.1515
Ha <i>et al.</i> [24]	$T = 0.0196H$	0.1700
IS 875 (Part 3)[25]	$T = 0.09H/\sqrt{D}$	0.2619
KBC [26]	$T = 0.073H^{0.75}$	0.1900
Lagomarsino [27]	$T = 0.018H$	0.1852
Tamura [28]	$T = 0.015H$	0.2222

4.2 Structural Damping Ratio (ζ_s)

From the perspective of structural response under dynamic loading, structural damping is a crucial parameter. Table 3 lists the various single value structural damping ratios of the numerous codal provisions.

Table 3. Structural Damping ratios of tall RC building

Code	Structural damping ratio(ζ_s)
ASCE 7-16 [22]	2%
AS/NZ1170 [29]	1%
Eurocode [23]	1.57%
ISO [30]	1.2%
IS 875 (Part 3)[25]	2%

5. Wind Parameters

5.1 Exponent of Mean Velocity Profile (α)

Exponent of mean velocity profile(α) is a pivotal parameter in defining the approaching wind profile. Equation (17) shows the power-law profile of approaching wind.

$$U(H) = U_{\text{ref}} \left(\frac{H}{H_{\text{ref}}} \right)^{\alpha} \quad (17)$$

Where, UH is the wind speed at height H, Href is the reference height taken as 10 meters. Uref is called as reference wind speed which is defined at the reference height. In this case Uref is considered as 25.2326 m/s. Href and Uref are kept constant, and only exponent of

mean wind velocity(α) is varied. Various international standards recommend the values of exponent of mean velocity profile for different types of terrain categories. The value of α for the urban terrain is shown in Table 4.

Table 4. Exponent of mean velocity profile for urban terrain

Code	Exponent of mean velocity profile for urban terrain (α)	Wind speed at the height of target building (U_H) in m/s
AIJ [31]	0.35	82.98
ASCE 7-16 [22]	0.25	59.05
GB 50009[13]	0.3	70
ISO [30]	0.40	98.36
NBCC [32]	0.36	85.84

5.2 Turbulence Intensity (I_H)

Turbulence intensity gives an understanding of wind turbulence in the approaching flow and it affects the effective wind loads on the structure. International codes have provided formulations to assess the turbulence intensity at the location of the building based on the terrain category parameters as presented in Table 5.

Table 5. Turbulence intensity profile and its parameters for urban terrain

Code	Turbulence intensity for urban terrain	Different parameters and their values for urban terrain	Turbulence Intensity in Percentage
ASCE 7-16 [22]	$I_z = c \left(\frac{10}{z}\right)^{1/6}$	$c=0.30,$ $\bar{z} = 0.6h$	18.53
AS/NZ1170 [29] (formulated)	$I_z = c \left(\frac{10}{z}\right)^d$	$c=0.40, d=0.24$	17.68
Eurocode [23]	$I_z = \left(\frac{1}{\ln(z/z_0)}\right)$	$z_0=1, z=h$	17.53
IS 875 (Part 3)[25]	$I_{z,4}$ $= 0.466 - 0.1358 \log_{10} \left(\frac{z}{z_{0,4}}\right)$	$z_{0,4} = 2, z=h$	17
ISO [30]	$I_z = \left(\frac{1}{\ln(z/z_0)}\right)$	$z_0=3, z=h$	21.71

5.3 Peak Factor for Resonant Response (g_R)

g_R is influenced by the averaging time (T) and the up-crossing rate (ν), which is nearly equivalent to the natural frequency of the structure under the assumption that the development is narrow banded Gaussian. Quan and Gu [16] used the peak factor related to averaging time 10-minutes (600 sec), so here, for the conformity, we have opted the international standards, which specifically use 10-min averaging time. Here, f_1 is fundamental natural frequency of the building. Quan and Gu [16] used the fundamental frequency as 0.2 Hz so for comparison of different peak background factor, fundamental frequency is kept constant as 0.2 Hz for all cases. Various codal provisions for estimating the peak factor for resonant response are presented in Table 6.

Table 6. Peak factor for resonant response for various codes and its magnitude at fundamental frequency 0.2 Hz

Code	Peak factor for resonant response (g_R)	$f = 0.20$ Hz
AIJ [31]	$g_R = \sqrt{2\ln(600f_1) + 1.2}$	3.2825
AS/NZ1170 [29]	$g_R = \sqrt{2\ln(600f_1)}$	3.0943
Eurocode [23]	$g_R = \sqrt{2\ln(600f_1) + \frac{0.6}{\sqrt{2\ln(600f_1)}}}$	3.2882
ISO [30]	$g_R = \sqrt{2\ln(600f_1) + \frac{0.577}{\sqrt{2\ln(600f_1)}}}$	3.2808
GB 50009[13]	2.5	2.5

5.4 Background Peak Factor (g_B)

Almost all codes use a single value for the background peak factor. The Japanese and European codes use the value of g_B same as g_R . Table 7 shows the background peak factor for the various codal provisions. In contrast to other codes, the Chinese code specifies a fixed value of 2.5 for g_B and g_R , leading to significantly lower values. There is no clear explanation for this choice.

Table 7. Background Peak factor for various codes

Code	Background Peak factor (g_B)
AIJ [31]	$g_B = g_R = 3.2825$
AS/NZ1170 [29]	3.7
Eurocode [23]	$g_B = g_R = 3.2882$
ISO [30]	3.4
GB 50009[13]	2.5

6. Methodology

Following the instructions of the section analytical method, a MATLAB code is developed in the present study to evaluate all the parameters and compute the across wind ESWL and responses. The MATLAB code is provided in Appendix A. The validation of the code is done by comparing the results with Quan and Gu [16] as shown in Fig. 2. The evaluation of parameters is conducted using a variety of international codes in order to understand the range of parameters. There is a total of six parameters, whose effect on wind load is studied. Out of six parameters, only one is varied at a time, while the other independent parameter remains constant. Table 8 contains the fixed values of parameters. The effect of each parameter on across wind load and response is analyzed.

7. Results and Discussion

7.1 Effect of Natural Frequency (f) of the Structure

The across wind load of the super tall building is calculated on different natural frequencies. Table 8 lists the parameters that are kept constant in this section. The provisions for determining natural frequencies according to various codes are presented in the section structural parameters. The calculation procedures for calculating the across-wind ESWL and response are succinctly discussed in the section analytical method. Figures 3(a)-(d) show the variation in ESWL, shear force, bending moment, and peak acceleration along the height of the building. Peak factor for resonant response (g_R) is dependent on fundamental natural frequency of the structure. Therefore, g_R is automatically varied

while varying the natural frequency in this case. The parameters other than these two are kept constant. The Eurocode [23] proposes the lowest natural frequency for the building, while IS 875 (Part 3)[25] recommends the highest. As per the Fig 3, it is evident that the results obtained are maximum for Eurocode [23], while the results for IS 875 (Part 3)[25] are the minimum. It is evident from the results that as the natural frequency of the building is decreasing, the across wind load and responses are increasing. It is happening because the background components are highly sensitive to reduced frequency (n) which is a function of natural frequency.

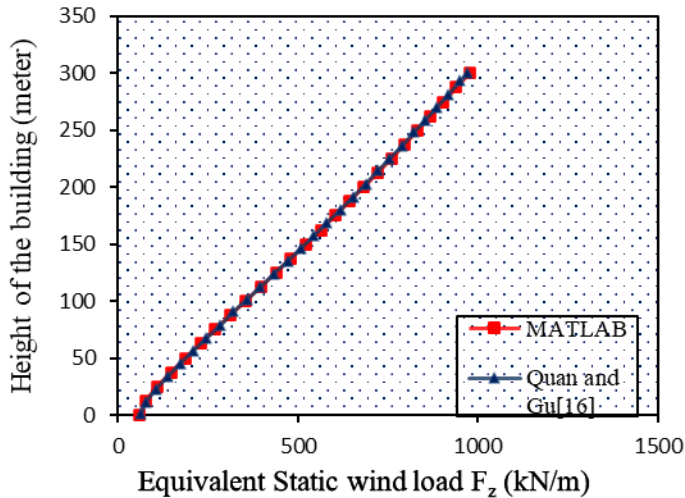


Fig.2 Comparison of Quan and Gu[16] and MATLAB results

Table 8. Fixed value of parameters.

Parameter	Value
Natural frequency(f) of the structure	0.20 Hz
Structural damping ratio (ζ_s)	1%
Exponent of mean velocity profile (α)	0.30
Turbulence intensity (I_H)	11%
Peak factor for resonant response (g_R)	3.281
Background peak factor (g_B)	3.5

7.2 Effect of Structural Damping Ratio (ζ_s)

In this section, the across wind load is calculated at different structural damping ratio (ζ_s) and keeping all the other parameters constant. As mentioned in Table 3, AS/NZ 1170 [29] recommends the lowest value of the structural damping ratio of the building, while ASCE 7-16 [22] and IS 875 (Part 3)[25] suggest the highest value. Fig. 4(a) -(d) delineates the variation of ESWL, shear force, bending moment, and peak acceleration along the building height. It can be observed from Fig 4(a)-(d) that AS/NZ 1170 [29] gives the maximum wind load. Since both ASCE 7-16 [22] and IS 875 (Part 3)[25] recommend the same, and high value of structural damping ratio, the across wind load is similar and minimum. A conclusion can be drawn that as the structural damping ratio increases the across wind load decreases. This study's findings agree with Wang et al. [33] and Li et al. [34], which found a decrease in cross-wind response as structural damping increased.

7.3 Effect of Exponent of Mean Velocity Profile (α)

Figure 5(a)-(d) illustrates the impact of wind velocities provided in Table 4 on the across wind loads and responses. Across wind load is maximum for ISO [30] because it has the maximum exponent value and due to this, it proposes the maximum wind velocity at height of target building. ASCE 7-16 [22] proposes the minimum value of exponent among other codes; hence the across wind load is minimum in this case. Based on Fig. 5 the conclusion can be drawn that as the wind speed increases across wind load and response also increases. Gu *et al.* [35] also concluded the same in their study. According to their statement, the susceptibility of the across-wind response is greater to the approaching wind speed as compared to the along-wind response. In general, longitudinal wind loads are more prominent at lower wind velocities, whereas transverse wind loads are predominant at higher velocities. The inherent frequencies of exceptionally tall structures are comparatively low, and the velocity of wind is greater at the uppermost tiers of the boundary layer. Consequently, the reduced frequency of a skyscraper at the wind speed for which it was designed may correspond to the reduced frequency at which the maximum force spectrum across the wind direction transpires.

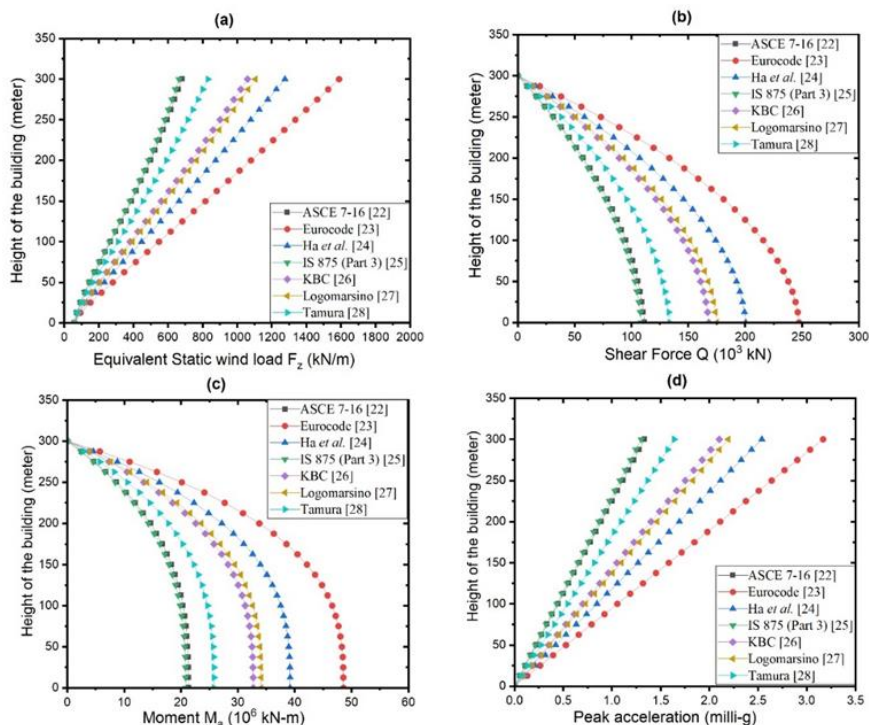


Fig. 3 ESWL, Shear Force, Moment and Peak acceleration along the height of the building for various natural frequencies

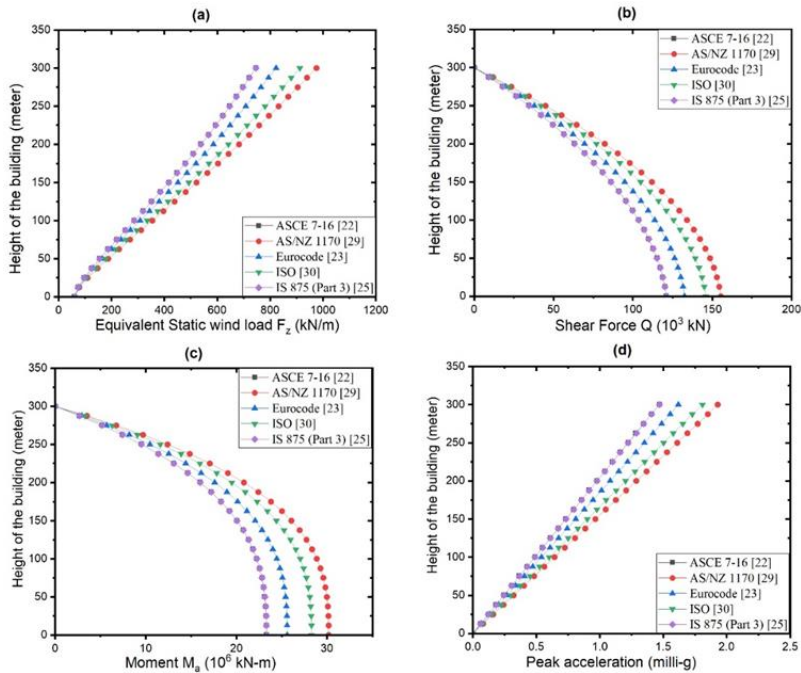


Fig.4 ESWL, Shear Force, Moment and Peak acceleration along the height of the building for various structural damping ratio

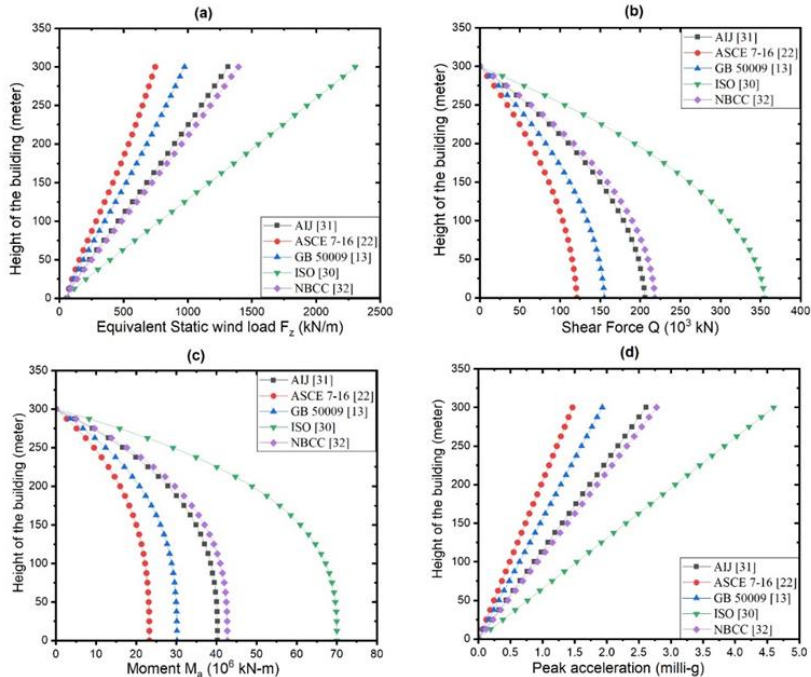


Fig. 5 ESWL, Shear Force, Moment and Peak acceleration along the height of the building for various exponent of mean velocity profile

7.4 Effect of Turbulence Intensity (I_H)

This section involves the calculation of the across wind load of tall building at different turbulence intensity values while keeping the other five parameters constant. Through the results obtained in the study, it can be inferred that turbulence intensity has a minimal effect on the across wind loads. The results collected from the various turbulence intensities produced similar outcomes. Table 9 exhibits the across wind load values (kN/m) from the analysis of five international codes. Cheng et al. [36] have previously deduced that the lift coefficient, an indicator of the across wind load, does not exhibit a correlation with changes in turbulence intensity. The current study has corroborated these findings. While the along-wind force spectrum primarily reflects the wind turbulence approaching the structure, the across-wind force spectrum is mostly influenced by vortex formation and flow separation. Therefore, the turbulence intensity has minimal impact on the across-wind response.

Table 9. Across wind ESWL of a 300 m super high-rise building at various turbulence intensity

Height	ASCE 7-16 [22]	AS/NZ1170 [29]	Eurocode [23]	IS 875 (Part 3) [25]	ISO [30]
0.00	60.54	60.54	60.54	60.54	60.54
12.50	77.98	77.98	77.99	77.99	77.98
25.00	110.16	110.17	110.17	110.18	110.15
37.50	147.89	147.90	147.91	147.92	147.88
50.00	187.96	187.98	187.98	188.00	187.94
62.50	229.20	229.22	229.22	229.24	229.17
75.00	271.08	271.10	271.11	271.13	271.05
87.50	313.31	313.34	313.34	313.37	313.27
100.00	355.68	355.72	355.72	355.76	355.64
112.50	398.05	398.09	398.10	398.13	398.00
125.00	440.28	440.32	440.33	440.37	440.23
137.50	482.25	482.30	482.31	482.35	482.19
150.00	523.86	523.91	523.92	523.97	523.80
162.50	565.02	565.07	565.08	565.14	564.95
175.00	605.63	605.69	605.71	605.76	605.56
187.50	645.65	645.71	645.73	645.79	645.57
200.00	685.02	685.09	685.10	685.17	684.94
212.50	723.72	723.79	723.81	723.88	723.63
225.00	761.76	761.83	761.85	761.92	761.66
237.50	799.15	799.23	799.25	799.33	799.05
250.00	835.98	836.06	836.08	836.16	835.87
262.50	872.34	872.43	872.45	872.53	872.22
275.00	908.38	908.48	908.50	908.59	908.26
287.50	944.31	944.41	944.43	944.53	944.18
300.00	980.37	980.47	980.50	980.60	980.24

7.5 Effect of peak factor for resonant response (g_R)

The study analyzed the across wind loads of a super tall building at various peak factors for resonant response (g_R) while holding the other five parameters constant (as shown in Table 8). The results were visualized in Fig. 6 (a)-(d), which displayed the variation of ESWL, shear force, bending moment, and peak acceleration along the height of the building. The findings from AIJ [31], ISO [30], and Eurocode [23] were quite similar. However, GB

50009 [13] showed the lowest across wind loads, primarily due to the lowest value of the resonant factor. It is observed that as the resonant factor increased, the across wind load also increased.

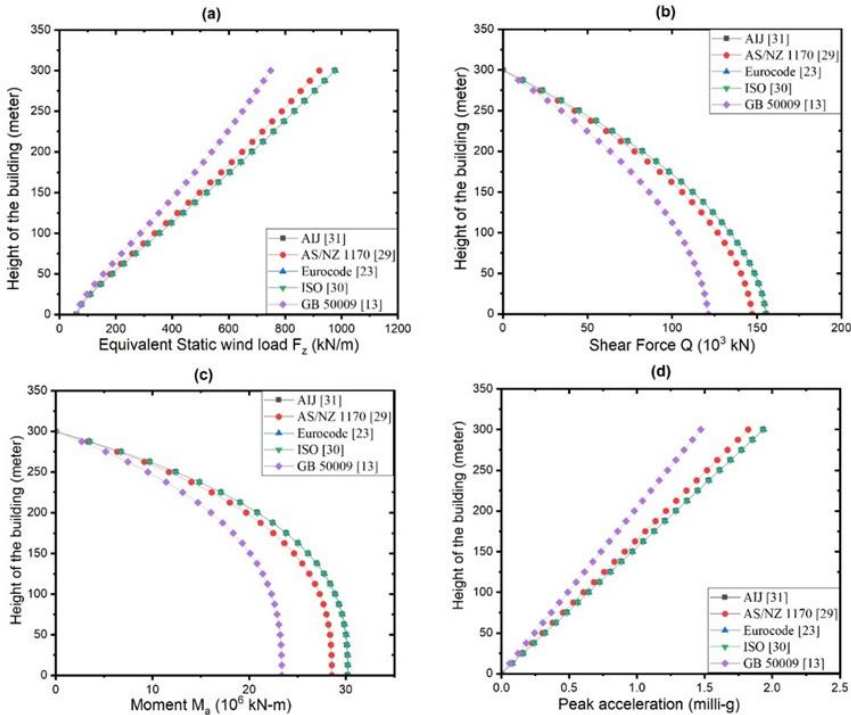


Fig.6 ESWL, Shear Force, Moment and Peak acceleration along the height of the building for g_R

7.6 Effect of Background Peak Factor (g_B)

The background response refers to a type of quasi-static response that occurs by variations in turbulence wind at low frequencies, which are too low to instigate any resonant response [37]. This section examines the across wind loads of the structure calculated at different background peak factor (g_B) and keeping the other five parameters constant. It can be seen from Fig.7(a)-(c) that effect of background peak factor on across wind load is minimum. Peak acceleration does not depend on the background peak factor (Equation 16). Therefore in Fig.7(d), all the codes produce equal peak acceleration.

7.7 Variations in the Across Wind Load Caused by Various Parameters

Variation of all the parameters with the maximum across wind ESWL is plotted in Fig. 8. A constant vertical axis of across wind ESWL is maintained for all the parameters. There is a rapid decrease in across wind load as the natural frequency increases. As the structural damping ratio increases the across wind load decreases. As the exponent of mean velocity profile increases, the across wind load also increases exponentially. Turbulence intensity does not influence the across wind load. As the peak factor for resonant response increases, the across wind load also increases. As the background peak factor increases the across wind load increases gradually. Out of the six parameters, the exponent of mean velocity profile affects the across wind load the most.

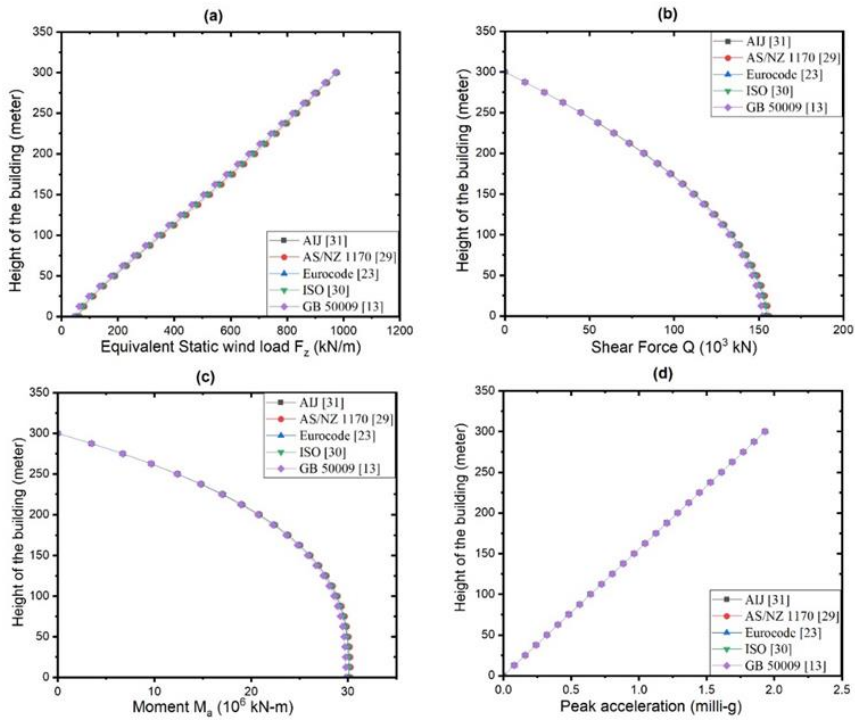


Fig. 7 ESWL, Shear Force, Moment and Peak acceleration along the height of the building for g_B

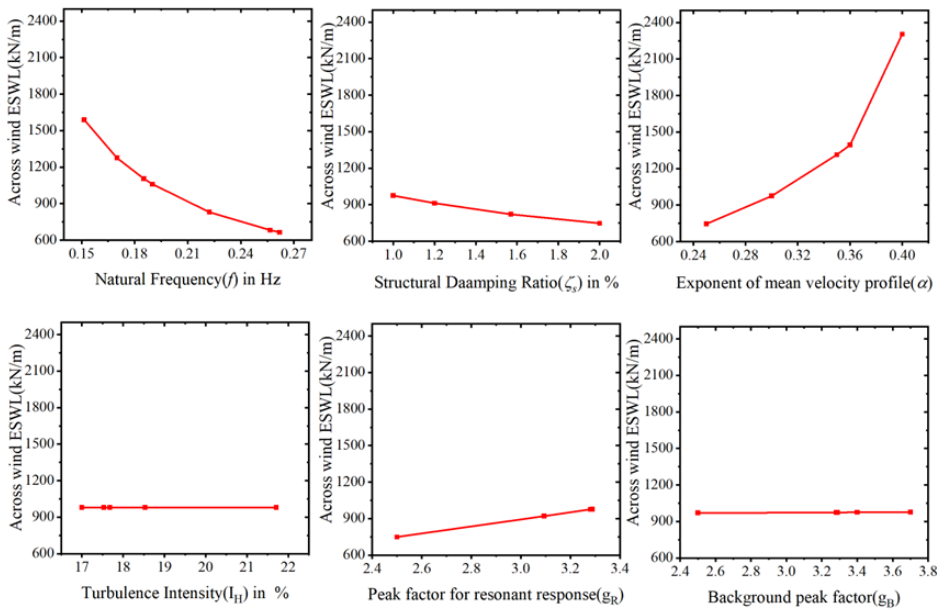


Fig.8 Variation of across wind load with various parameters

8. Conclusions

When designing a super high-rise building, it is crucial to take into account the wind loads it will be subjected to, particularly the across-wind load. Both wind and structural parameters heavily influence this type of load, and their impact on the across-wind load is still uncertain. This paper studies the effect of wind and structural parameters on across wind load. A hypothetical super high-rise building of 300 m in height and square cross-section, assumed to be located in urban terrain, is selected for analysis. Evaluation of the parameters is carried out in accordance with several international standards. To determine the across wind ESWL and responses, a MATLAB code is developed. The results are presented in the form of ESWL, Shear Force, Bending Moment, and Peak Acceleration. The following are critical outcomes of the present study.

- The results clearly show that as the natural frequency changes from 0.1515Hz to 0.2619 Hz, there is a change in the across wind ESWL from 1589kN/m to 664 kN/m. It is because the background components of the building are highly responsive to the natural frequency.
- The exponent of mean velocity profile (α) influences the cross wind load the most compared to other parameters. As the α changes from 0.36 to 0.4, there is a 65% increase in wind load. At high wind speed, there is an intense across-wind response.
- This study has demonstrated that when the structural damping ratio increases, there is a decrease in the cross-wind load. As the structural damping ratio increases from 1% to 2%, the across-wind ESWL decreases from 975 to 746kN/m.
- Across wind load is minimally affected by the turbulence intensity of the surrounding wind. As the turbulence intensity changes from 17% to 21.71%, the across wind ESWL remained unchanged as 980kN/m
- The peak factor for resonant response (g_R) affects the cross wind loads more in comparison to the background peak factor (g_B), and Peak acceleration is independent of the Background peak factor (G_B). As the g_R changes from 2.5 to 3.2882, the cross wind ESWL, the across wind ESWL increases from 748 kN/m to 977 kN/m. The background peak factor(g_B) changes from 2.5 to 3.7, there is a small increase in across wind ESWL as 971kN/m to 976kN/m.

This study substantially helps to understand the variation in wind loading due to the variability of the key parameters involved. It is crucial to have precise estimations of wind and structural parameters. It is essential to accurately determine these parameters to avoid underestimating or overestimating the wind load exerted on a structure, which may lead to flawed load calculations and faulty building design. Additionally, wind tunnel studies and full-scale experiments should be conducted to study the same in greater detail.

References

- [1] Davenport AG. Gust loading factors. Journal of the Structural Division. 1967;93(3):11-34. <https://doi.org/10.1061/JSDEAG.0001692>
- [2] Chen X, Kareem A. Dynamic wind effects on buildings with 3D coupled modes: Application of high frequency force balance measurements. Journal of Engineering Mechanics. 2005;131(11):1115-25. [https://doi.org/10.1061/\(ASCE\)0733-9399\(2005\)131:11\(1115\)](https://doi.org/10.1061/(ASCE)0733-9399(2005)131:11(1115))
- [3] Liang S, Liu S, Li QS, Zhang L, Gu M. Mathematical model of acrosswind dynamic loads on rectangular tall buildings. Journal of Wind Engineering and Industrial Aerodynamics. 2002;90(12-15):1757-70. [https://doi.org/10.1016/S0167-6105\(02\)00285-4](https://doi.org/10.1016/S0167-6105(02)00285-4)

- [4] Tallin A, Ellingwood B. Analysis of torsional moments on tall buildings. *Journal of wind engineering and industrial aerodynamics*. 1985;18(2):191-5. [https://doi.org/10.1016/0167-6105\(85\)90097-2](https://doi.org/10.1016/0167-6105(85)90097-2)
- [5] Cheung JC, Melbourne WH. Torsional moments of tall buildings. *Journal of Wind Engineering and Industrial Aerodynamics*. 1992;42(1-3):1125-6. [https://doi.org/10.1016/0167-6105\(92\)90119-U](https://doi.org/10.1016/0167-6105(92)90119-U)
- [6] Lythe GR, Surry D. Wind-induced torsional loads on tall buildings. *Journal of Wind Engineering and Industrial Aerodynamics*. 1990;36:225-34. [https://doi.org/10.1016/0167-6105\(90\)90307-X](https://doi.org/10.1016/0167-6105(90)90307-X)
- [7] Gu M, Quan Y. Across-wind loads and effects of super-tall buildings and structures. *Science China Technological Sciences*. 2011;54:2531-41. <https://doi.org/10.1007/s11431-011-4543-5>
- [8] Gu M, Quan Y. Across-wind loads of typical tall buildings. *Journal of Wind Engineering and Industrial Aerodynamics*. 2004;92(13):1147-65. <https://doi.org/10.1016/j.jweia.2004.06.004>
- [9] Zhou Y, Kareem A, Gu M. Equivalent static buffeting loads on structures. *Journal of Structural Engineering*. 2000;126(8):989-92. [https://doi.org/10.1061/\(ASCE\)0733-9445\(2000\)126:8\(989\)](https://doi.org/10.1061/(ASCE)0733-9445(2000)126:8(989))
- [10] Gu M, Zhou Y, Zhang F, Xiang HF. Dynamic responses and equivalent wind loads of the Jin Mao Building in Shanghai. In *Proceedings of the tenth international conference on wind engineering, Copenhagen, Denmark, Vol. 3*, pp. 1497-504,1999.
- [11] Li QS, Xiao YQ, Fu JY, Li ZN. Full-scale measurements of wind effects on the Jin Mao building. *Journal of Wind Engineering and Industrial Aerodynamics*. 2007;95(6):445-66. <https://doi.org/10.1016/j.jweia.2006.09.002>
- [12] Zheng WZ, Alex PT. Comparative study of along-wind and across-wind loads on tall buildings with different codes. *Proceedings of 14th international Symposium on Structural Engineering*. Beijing, China, 723-728, 2016.
- [13] Ministry of Housing and Urban-Rural Development of the People's Republic of China. GB 50009-2012 Load Code for the Design of Building Structures. 2012.
- [14] Kwon DK, Kareem A. Comparative study of major international wind codes and standards for wind effects on tall buildings. *Engineering Structures*. 2013;51:23-35. <https://doi.org/10.1016/j.engstruct.2013.01.008>
- [15] Holmes J, Tamura Y, Krishna P. Comparison of wind loads calculated by fifteen different codes and standards, for low, medium and high-rise buildings. In *11th Americas conference on wind engineering, San Juan, Puerto Rico, 1-10, 2009*.
- [16] Quan Y, Gu M. Across-wind equivalent static wind loads and responses of super-high-rise buildings. *Advances in Structural Engineering*. 2012;15(12):2145-55. <https://doi.org/10.1260/1369-4332.15.12.2145>
- [17] Singh A, Mandal S. Effect of plan and height aspect ratios on along wind and across wind loads on super high rise buildings. *Jordan Journal of Civil Engineering*. 2022;16(2):335-354.
- [18] Sharma A, Mittal H, Gairola A. Mitigation of wind load on tall buildings through aerodynamic modifications. *Journal of Building Engineering*. 2018;18:180-94. <https://doi.org/10.1016/j.jobe.2018.03.005>
- [19] Jafari M, Alipour A. Methodologies to mitigate wind-induced vibration of tall buildings: A state-of-the-art review. *Journal of Building Engineering*. 2021;33:1-25. <https://doi.org/10.1016/j.jobe.2020.101582>
- [20] Quan Y, Gu M, Tamura Y. Experimental evaluation of aerodynamic damping of square super high-rise buildings. *Wind & structures*. 2005;8(5):309-24. <https://doi.org/10.12989/was.2005.8.5.309>
- [21] Xu YL, Kwok KC. Mode shape corrections for wind tunnel tests of tall buildings. *Engineering Structures*. 1993;15(5):387-92. [https://doi.org/10.1016/01410296\(93\)90042-3](https://doi.org/10.1016/01410296(93)90042-3)

- [22] American Society of Civil Engineers. ASCE/SEI 7-16. Minimum design loads and associated criteria for buildings and other structures. American Society of Civil Engineers. 2016.
- [23] European Committee for Standardization (C.E.N.). Eurocode 1: Actions on Structures—Part 1–4: General Actions—Wind Actions; pr EN 1991-1-4.6; European Committee for Standardization (C.E.N.): Brussels, Belgium. 2004.
- [24] Ha T, Shin SH, Kim H. Damping and natural period evaluation of tall RC buildings using full-scale data in Korea. *Applied Sciences*. 2020;10(5):1-16. <https://doi.org/10.3390/app10051568>
- [25] IS 875 (Part 3): 2015, Bureau of Indian Standards, Indian Standard Code of Practice for design loads (other than earthquake) for buildings and structures. Part 3 – Wind loads, 2015.
- [26] Architectural Institute of Korea. Korean Building Code (KBC). Structural 2009; Ministry of Construction and Transportation of Korea: Seoul, Korea. 2009.
- [27] Lagomarsino S. Forecast models for damping and vibration periods of buildings. *Journal of Wind Engineering and Industrial Aerodynamics*. 1993;48(2-3):221-39. [https://doi.org/10.1016/0167-6105\(93\)90138-E](https://doi.org/10.1016/0167-6105(93)90138-E)
- [28] Tamura Y. Damping in buildings for wind resistant design. International Symposium on Wind and Structures for the 21st Century, Cheju, Korea, 115-130, 2000.
- [29] Australia/New Zealand (AS/NZS). Australian/New Zealand Standards, Structural Design Actions—Part 2, Wind Actions. AS/NZS 1170.2:2011; Standards Australia: Sydney, Australia, 2011
- [30] ISO 4354 (E) Second Edition: Wind Actions on Structures; International Organization for Standardization: Geneva, Switzerland, 2009.
- [31] Architecture Institute of Japan (AIJ).: Recommendations for loads on buildings. Architectural Institute of Japan. Tokyo, Japan. 2004 (In Japanese)
- [32] NBCC.: National building Code of Canada. National Research Council of Canada, Ottawa, Canada. 2020.
- [33] Wang M, Nagarajaiah S, Sun FF. A novel crosswind mitigation strategy for tall buildings using negative stiffness damped outrigger systems. *Structural Control and Health Monitoring*. 2022;29(9):2988. <https://doi.org/10.1002/stc.2988>
- [34] Li SY, Liu M, Li HX, Hui Y, Chen ZQ. Effects of structural damping on wind-induced responses of a 243-meter-high solar tower based on a novel elastic test model. *Journal of Wind Engineering and Industrial Aerodynamics*. 2018;172:1-11. <https://doi.org/10.1016/j.jweia.2017.10.027>
- [35] Gu M, Su L, Quan Y, Huang J, Fu G. Experimental study on wind-induced vibration and aerodynamic mitigation measures of a building over 800 meters. *Journal of Building Engineering*. 2022 Apr 1;46:103681. <https://doi.org/10.1016/j.jobbe.2021.103681>
- [36] Cheng CM, Lu PC, Chen RH. Wind loads on square cylinder in homogeneous turbulent flows. *Journal of Wind Engineering and Industrial Aerodynamics*. 1992 ;41(1-3):739-49. [https://doi.org/10.1016/0167-6105\(92\)90490-2](https://doi.org/10.1016/0167-6105(92)90490-2)
- [37] Holmes JD. Resonant dynamic response and effective static load distributions. *Wind loading of structures*, 3rd edition, New York CRC press, 2018: 113-148, ISBN 1978-1-4822-2922-6

Appendix A: MATLAB Code for Calculation of across wind ESWL

```

H=300;
pp=H/24;
h=[0,pp/H,(2*pp/H),(3*pp/H),(4*pp/H),(5*pp/H),(6*pp/H),(7*pp/H),(8*pp/H),(9*pp/H),(10*pp/H),(11*pp/H),(12*pp/H),(13*pp/H),(14*pp/H),(15*pp/H),(16*pp/H),(17*pp/H),(18*pp/H),(19*pp/H),(20*pp/H),(21*pp/H),(22*pp/H),(23*pp/H),1];
B=(300/6);
D=(300/6);
f1=1/T; %T=H^0.9/43.5%, %(Euro)T=0.022H
beta=1;
zetas=.01; %2,1,1.57,1.2,2%
rhoS=200;
mz=(B*D*rhoS);
syms k real
Mi=int(mz/(H^2))*k^2,k,[0 H]);
alpha=0.3;
Ih=0.11;
Uh=82.98;
Us=Uh/(f1*B);
wh=2996; % wh=(0.5*1.225*(Uh^2))%
alphadb=D/B;
alphaw=4.2-4*exp(3.7-60*Ih);
Cmbo=0.182-0.019*(alphadb^-2.54)+0.054*(alphaw^-0.91);
gr=sqrt(2*log(600*f1))+(0.5772/sqrt(2*log(600*f1))); % gr=2.5;%
phi=1;
alphahr=H/(sqrt(B*D));
fp=(10^-5)*(191-9.48*alphaw+1.28*alphahr+alphahr*alphaw)*(68-21*alphadb+3*alphadb*alphadb);
Sp=(0.1*(alphaw^-0.4)-0.0004*exp(alphaw))*(0.84*alphahr-2.12-0.05*alphahr*alphahr)*(0.422+(alphadb^-1)-0.08*(alphadb^-2));
neta=(1+0.00473*exp(1.7*alphaw))*(0.065+exp(1.26-0.63*alphahr))*(exp(1.7-(3.44/alphadb)));
lambda=(-0.8+0.06*alphaw+0.0007*exp(alphaw))*((-alphahr^0.34)+0.00006*exp(alphahr))*(0.414*alphadb+1.67*(alphadb^-1.23));
n=f1*B/Us;
Sm=(Sp*neta*(n/fp)^lambda)/((1-(n/fp)^2)^2+(neta*(n/fp)^2));
zetaaa=(0.0025*(1-(Us/9.8)^2)*(Us/9.8)+0.000125*(Us/9.8)^2)/((1-(Us/9.8)^2)^2+0.0291*(Us/9.8)^2);
%zetaaa=0.0040;
gb=3.5;
ptotal=zeros(1,25);
atotal=zeros(1,25);
for i=1:25
GbZ=((0.65+1.3*h(1,i)+7*(h(1,i))^2-7.5*(h(1,i))^3)*gb*Cmbo);
%GbZ=((0.65+1.3*h+7*h^2-7.5*h^3)*gb*Cmbo);
Grz=(H*mz/Mi)*(h(1,i))^beta*gr*(sqrt(pi*phi*Sm/(4*(zetas+zetaaa))));
%Grz=(H*mz/Mi)*h*gr*(sqrt(pi*phi*Sm/(4*(zetas+zetaaa))));
pz=wh*B*(sqrt(GbZ^2+Grz^2));
az=(H/Mi)*(h(1,i))^beta*gr*B*wh*(sqrt(pi*phi*Sm/(4*(zetas+zetaaa))));
ptotal(1,i)=pz/1000;
atotal(1,i)=az;
end

```